The Microbial Opsin Family of Optogenetic Tools

Feng Zhang,[1,2,9,*] Johannes Vierock,[3,9] Ofer Yizhar,[4] Lief E. Fenno,[5] Satoshi Tsunoda,[3] Arash Kianianmomeni,[3] Matthias Prigge,[3] Andre Berndt,[3] John Cushman,[6] Jürgen Polle,[7] Jon Magnuson,[8] Peter Hegemann,[3,*] and Karl Deisseroth[5,*]

[1]Broad Institute of MIT and Harvard, Cambridge, MA 02142, USA
[2]McGovern Institute for Brain Research, Department of Brain and Cognitive Sciences, Massachusetts Institute of Technology, Cambridge, MA 02139, USA
[3]Institute of Biology, Experimental Biophysics, Humboldt-Universität zu Berlin, Invalidenstrasse 42, D-10115 Berlin, Germany
[4]Department of Neurobiology, Weizmann Institute of Science, Rehovot 76100, Israel
[5]Howard Hughes Medical Institute, CNC Program, Departments of Bioengineering and Psychiatry, Stanford University, Stanford, CA 94305, USA
[6]Department of Biochemistry and Molecular Biology, University of Nevada, Reno, NV 89557, USA
[7]Department of Biology, Brooklyn College, The City University of New York, Brooklyn, NY 11210, USA
[8]Chemical & Biological Processes Development Group, Pacific Northwest National Laboratory, Richland, WA 99352, USA
[9]These authors contributed equally to this work
*Correspondence: zhang_f@mit.edu (F.Z.), hegemape@rz.hu-berlin.de (P.H.), deissero@stanford.edu (K.D.)
DOI 10.1016/j.cell.2011.12.004

The capture and utilization of light is an exquisitely evolved process. The single-component microbial opsins, although more limited than multicomponent cascades in processing, display unparalleled compactness and speed. Recent advances in understanding microbial opsins have been driven by molecular engineering for optogenetics and by comparative genomics. Here we provide a Primer on these light-activated ion channels and pumps, describe a group of opsins bridging prior categories, and explore the convergence of molecular engineering and genomic discovery for the utilization and understanding of these remarkable molecular machines.

Introduction

Diverse and elegant mechanisms have evolved to enable organisms to harvest light for a variety of survival functions, including energy generation and the identification of suitable environments. A major class of light-sensitive protein consists of 7-transmembrane (TM) rhodopsins that can be found across all kingdoms of life and serve a diverse range of functions (Figure 1). Many prokaryotes employ these proteins to control proton gradients and to maintain membrane potential and ionic homeostasis, and many motile microorganisms have evolved opsin-based photoreceptors to modulate flagellar beating or flagellar motor rotation and thereby direct phototaxis toward environments with optimal light intensities for photosynthesis.

Owing to their structural simplicity (both light-sensing and effector domains are encoded within a single gene) and fast kinetics, microbial opsins can be treated as precise and modular photosensitization components for introduction into non-light-sensitive cells to enable rapid optical control of specific cellular processes. In recent years, the development of cellular perturbation tools based on these and other light-sensitive proteins has resulted in a technology called optogenetics (Deisseroth, 2011; Deisseroth et al., 2006), which refers to the integration of genetic and optical control to achieve gain or loss of function of precisely defined events within specified cells of living tissue. Details of practical application for neuroscience have been recently summarized elsewhere (Yizhar et al., 2011a; Zhang et al., 2010).

The experimental potential of optogenetics has triggered a surge of genome prospecting and molecular engineering to expand the repertoire of tools and generate new classes of functionality, all of which have catalyzed further mechanistic studies of microbial proteins such as channelrhodopsins (ChRs). Here we provide a Primer on the structural and functional diversity of the microbial opsins, introduce an array of new sequences that inform mechanistic understanding of function, and explore resulting inferences into the principles of operation of this widespread and remarkably evolved class of proteins.

Fundamentals

Each opsin protein requires the incorporation of retinal, a vitamin A-related organic photon-absorbing cofactor, to enable light sensitivity; this opsin-retinal complex is referred to as rhodopsin. The retinal molecule is covalently fixed in the binding pocket within the 7-TM helices and forms a protonated retinal Schiff base (RSBH[+]; Figure 2A) with a conserved lysine residue located on TM helix seven (TM7). The ionic environment of the RSBH[+], heavily influenced by the residues lining the binding pocket, dictates the spectral characteristics of each individual protein; upon absorption of a photon, the retinal chromophore isomerizes and triggers a series of structural changes leading to ion transport, channel opening, or interaction with signaling transducer proteins (discussed below).
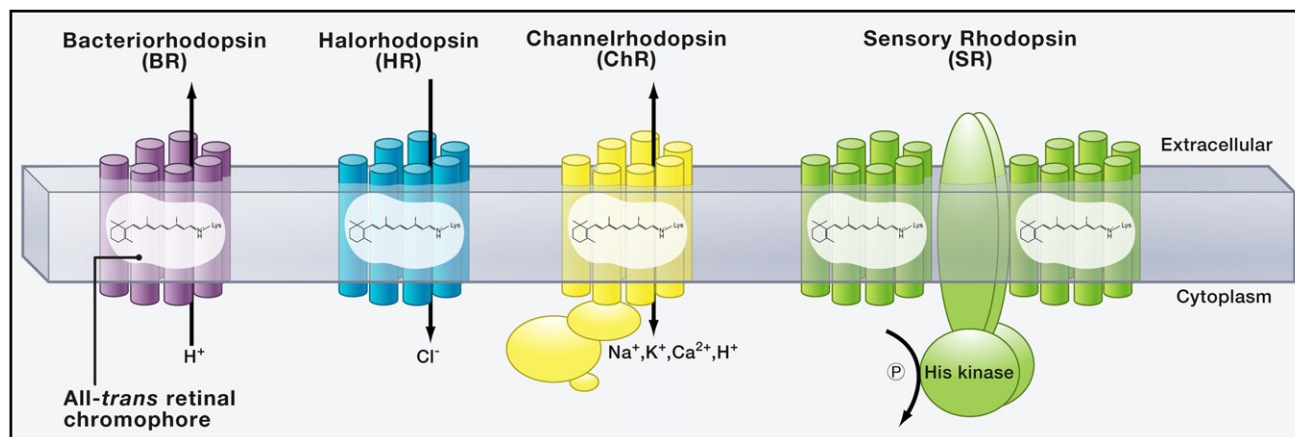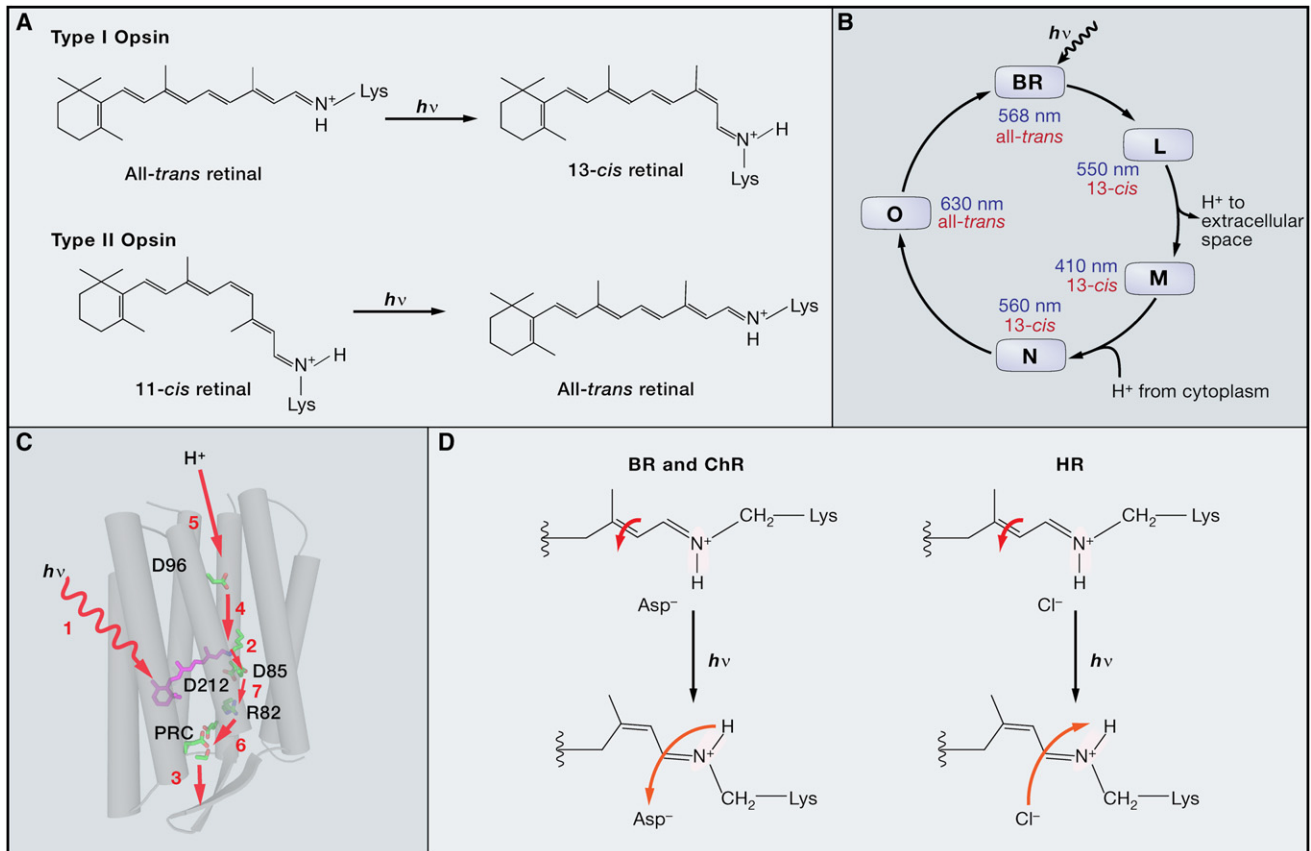
Figure 1. Type I Microbial Rhodopsins
BR (and PRs) pump protons from the cytoplasm to the extracellular medium, and HRs pump chloride into the cytoplasm; all three hyperpolarize the cell. SRs lack TM ion transport in the presence of the His kinase transducer protein Htr; and algal ChRs conduct cations across the membrane in both directions but always along the electrochemical gradient of the transported ions. In SRs and ChRs, proton translocation within the protein is linked to efficient photocycle progression, but these protons are not necessarily exchanged between the intra- and extracellular spaces.

Opsin genes are divided into two distinct superfamilies: microbial opsins (type I) and animal opsins (type II) (Spudich et al., 2000). Although both opsin families encode 7-TM structures (Luecke et al., 1999; Palczewski et al., 2000), sequence homology between the two families is practically nonexistent; homology within families, however, is high (25%–80% sequence similarity; Man et al., 2003). Type I opsin genes are found in prokaryotes, algae, and fungi and control diverse functions including phototaxis, energy storage, development, and retinal biosynthesis (Spudich, 2006). Type I opsins utilize the all-*trans* isomer of retinal, which isomerizes to the 13-*cis* configuration upon photon absorption (Figure 2A, top). The activated retinal molecule in type I rhodopsins remains associated with its opsin protein partner and thermally reverts to the all-*trans* state while maintaining a covalent bond to its protein partner (Haupts et al., 1997). This reversible reaction occurs rapidly and is critical for allowing microbial rhodopsins to modulate neuronal activity at high frequencies when used as optogenetic tools (Boyden et al., 2005; Zhang et al., 2006, 2007a; Ishizuka et al., 2006); fortuitously, mammalian brains, and indeed the vertebrate tissues thus far examined, contain sufficient levels of retinal so that additional retinal does not need to be supplemented to achieve optical control (Zhang et al., 2006).

In contrast, type II opsin genes are present only in higher eukaryotes and are mainly responsible for vision (Sakmar, 2002). A small fraction of type II opsins also play roles in circadian rhythm and pigment regulation (Sakmar, 2002; Shichida and Yamashita, 2003). Type II opsins primarily function as G protein-coupled receptors (GPCRs) and appear to all use the 11-*cis* isomer of retinal (or derivatives) for photon absorption (Figure 2A, bottom). Upon illumination, 11-*cis* retinal isomerizes into the all-*trans* configuration and initiates protein-protein interactions (not ion flux) that trigger the visual phototransduction second messenger cascade. Unlike the situation in type I rhodopsins, here the retinal dissociates from its opsin partner after isomerization into the all-*trans* configuration, and a new 11-*cis* retinal must be recruited. Due to these chromophore turnover reactions and the requirement for interaction with downstream biochemical signal transduction partners, type II opsins effect cellular changes with slower kinetics compared to type I opsins.

The power of using microbial opsins to modulate neuronal electrical activity has also stimulated strong interest in using light to control biochemical events in cells. Although not the focus here, it is worth noting that structure-function work in type II vertebrate opsins from many laboratories (such as Kim et al., 2005) inspired the design of synthetic opsins for controlling specific biochemical events in freely moving mammals. By replacing the intracellular loops of bovine rhodopsin with the intracellular loops from GPCRs, an expanding family of synthetic rhodopsins called optoXRs has enabled optical control of Gs, Gq, or Gi signaling in neuronal settings (Airan et al., 2009; Oh et al., 2010). It is also noteworthy that several groups have expanded control of intracellular signaling by engineering non-opsin-based light-regulated proteins to modulate general second messengers such as cAMP and cGMP (Schröder-Lang et al., 2007). For example, the photoactivated adenylyl cyclases (PACs) can be so employed and use the ubiquitous FAD as a cofactor for photoactivation, although early efforts using PACs from *Euglena gracilis* were hampered by a combination of high levels of basal activity in the dark, poor protein solubility, and large (~3 kbp) transgene size (Schröder-Lang et al., 2007). More recently, a smaller PAC derivative with lower dark activity from the soil bacterium *Beggiatoa* has been shown in neurons and *Drosophila* to alter membrane currents and influence behavior (Stierl et al., 2011). Yet the microbial opsins remain remarkable for both (1) unitary encoding of light sensation and final effector capability by a single compact gene and (2) virtually zero dark activity, along with millisecond-scale response to well-tolerated wavelengths and intensities of light. These core properties have provided a foundation for, and motivated, further investigation and engineering.

Figure 2. Photoreaction Mechanism

(A) Light-mediated isomerization of the retinal Schiff base (RSB). Top: retinal in the all-*trans* state, as found in the dark-adapted state of microbial rhodopsins and in the light-activated forms of type II rhodopsins of higher eukaryotes. The absorption of a photon converts the retinal from the all-*trans* to the 11-*cis* configuration. Bottom: 11-*cis* retinal is found only in type II rhodopsins, where it binds to the opsin in the dark state before isomerizing to the all-trans position after photon absorption.

(B) The photocycle of BR is initiated from the dark state where photon absorption activates a sequence of photochemical reactions and structural changes represented by the indicated photointermediates. Also shown is the configuration of the RSB in each step (in red) and the wavelength at which each intermediate maximally absorbs light (in blue).

(C) Summary of proton transport reactions during the BR photocycle. Photon absorption (1) initiates the conformational switch in the RSB, leading to transfer of a proton to Asp85 (2), release of a proton from the proton release complex (PRC, 3), reprotonation of the RSB by Asp96 (4), uptake of a proton from the cytoplasm to reprotonate Asp96 (5), and the reprotonation of the PRC from Asp85 (6), followed by a final proton transfer from D85 to R82 (7).

(D) Light-induced switching of dipole orientation in response to photon absorption in BR, ChR, and HR. In BR and the ChRs, the configuration switch triggers the transfer of the RSB proton to Asp85/Glu123 (for BR/ChR2, respectively). In HR, dipole switching facilitates the transfer of a Cl$^-$ ion from the cavity formed between the RSB and Thr143 to a Cl$^-$ binding site cytoplasmic to the RSB, enabling the key transport steps of these transporters. Curved arrows indicate isomerization (top row) and ion movement (bottom row).

Light-Activated Ion Pumps: Bacteriorhodopsin, Proteorhodopsin, and Halorhodopsin

Bacteriorhodopsin (BR) was first described as a single-component TM protein capable of translocating protons from the intracellular to the extracellular space (Oesterhelt and Stoeckenius, 1971). Haloarchaea express BR at high levels under low-oxygen conditions to maintain a proton gradient across the cellular membrane to drive ATP synthesis and maintain cellular energetics in the absence of respiration (Michel and Oesterhelt, 1976; Racker and Stoeckenius, 1974). During the proton translocation process, BR undergoes a cascade of photointermediate states, and each state can be identified by a distinct spectral signature (Lanyi, 2004). Photon absorption by BR first initiates the isomerization of the bound retinal from the all-*trans* to the 13-*cis* configuration (Figures 2A and 2B), thereby triggering a series of proton-transfer reactions that constitute the proton translocation mechanism (Figure 2C). This proton transport process, like chloride transport in halorhodopsins, is elegantly evolved to be (necessarily) spatially discontinuous to prevent passive back-diffusion of the ion down the gradient. Internal proton translocation begins when retinal isomerization triggers a conformational change in the protein and shifts the dipole of the RSBH$^+$. This dipole shift raises the pK$_a$ of the RSB, thereby resulting in the release of the proton to its nearby acceptor D85 (Figure 2D), and proton movement triggers additional changes in the protein. In the BR pump, the proton is released to the extracellular milieu via a proton release site defined by two surface glutamates. The RSB then indirectly absorbs a second proton from the cytoplasm, such that the photocycle can repeat with absorption of

another photon. In sensory rhodopsins (SRs) the internal proton transfer and subsequent structural changes trigger conformational changes in the transducer molecule (Htr) interacting with the rhodopsin. Certain aspects of the internal proton translocation process are conserved across many type I opsins; for example, locations of the carboxylate Schiff base proton acceptor and donor on the third TM helix are conserved across type I proton pumps.

BR-type proton-pumping opsins have been found across other kingdoms of life; for example, proteorhodopsins (PRs) have been found in marine proteobacteria with photocycles similar to that of BR (Váró et al., 2003). Because marine PRs share a high degree of sequence similarity across species and have action spectra that are tuned according to the ocean depth and latitude of their origin, several groups have explored genomic approaches to understand opsin spectral tuning (Man et al., 2003). Interestingly, absorption variance between blue and green wavelengths can depend on a single amino acid residue (Béjà et al., 2001; Man et al., 2003), but attempts to transfer mutations conferring spectral tuning from PR to other microbial opsins have met with limited success (Yoshitsugu et al., 2009). More extensive high-resolution crystal structures and molecular dynamics/molecular modeling of PRs, fungal opsins, and BRs may provide an opportunity to deepen understanding and extend functionality.

A BR-type proton pump called Archaerhodopsin-3 (initially identified by Ihara et al., 1999) has been shown to allow detection of voltage transients in neurons through generation of a voltage-dependent optical signal (Kralj et al., 2011); although it remains to be seen whether this functionality will be of utility in vivo, this class of experiment represents a potentially interesting value for the microbial opsins in neuroscience. The same protein (Archaerhodopsin-3) is also capable of generating hyperpolarizing currents that can be used to inhibit neural activity (Chow et al., 2010), as with other BR-type proton pumps (and indeed BR itself, optimized for mammalian expression; Gradinaru et al., 2010); however, the efflux of protons elicited by all of these proton pumps under typical steady-illumination experimental conditions will result in decreased extracellular pH. A distinct class of outward current-generating archaeal opsins known as halorhodopsins (HRs) (Matsuno-Yagi and Mukohata, 1977) instead use chloride as the charge carrier. HRs control gradients across the cell membrane by transporting chloride ions from the extracellular medium into the cell (Bamberg et al., 1984; Schobert and Lanyi, 1982). The primary photocycle, although qualitatively similar to that of BR, does not show RSBH⁺ deprotonation (Essen, 2002; Oesterhelt et al., 1985) due to a single amino acid substitution of the Asp acceptor with Thr. Therefore after the light-induced retinal isomerization and RSBH⁺ dipole switch, the proton cannot be released due to the absence of an appropriate acceptor. Instead, a Cl⁻ ion already present in the HR protein is transported from the external side of the RSBH⁺ chromophore to the internal side (Figure 2D) and is subsequently released into the intracellular space (Kolbe et al., 2000).

An experimental screen (Zhang et al., 2007b) revealed that the best known HR (from *Halobacterium salinarum*) failed to maintain stable photocurrents when expressed heterologously, whereas the HR from the less halophilic Egyptian *Natronomonas pharaonis* (NpHR) (initially identified by Lanyi et al., 1990; Scharf

and Engelhard, 1994) was capable of blocking animal (*C. elegans*) behavior by hyperpolarizing neurons with electrogenic inward Cl⁻ currents. Pump desensitization is modest, allowing stable, step-like currents over many tens of minutes in response to steady yellow light, but due to the stoichiometry of only one transported ion per photocycle (true for all light-driven pumps), robust expression and fast photocycles are required. Increased heterologous membrane expression can be achieved with addition of trafficking signals from mammalian membrane proteins (Gradinaru et al., 2008), and ultimately this version allowed the first optogenetic inhibition of behavior in mammals (Witten et al., 2010; reviewed in Yizhar et al., 2011a). Moreover, by significantly increasing the number of HR molecules on the neuronal membrane, NpHR (in this case, eNpHR3.0)-expressing neurons can even be inhibited by 680 nm far-red light, which is far from the action spectrum peak (Gradinaru et al., 2010).

Additional retinal-binding proteins have been identified from *Halobacterium salinarum* as behaviorally relevant photosensors (Hildebrand and Dencher, 1975; Takahashi et al., 1985), such as sensory rhodopsins SRI (Bogomolni and Spudich, 1982; Hildebrand and Dencher, 1975; Takahashi et al., 1985) and SRII, initially termed phoborhodopsin (Tomioka et al., 1986) or P480 (Marwan and Oesterhelt, 1987). The photocycle of SRs is similar to that of BR with analogous internal proton movements (Spudich, 1998; Spudich and Bogomolni, 1984), except that light-initiated conformational changes of the opsin are used to activate a closely associated transducer molecule Htr (Figure 1D) (Büldt et al., 1998; Chen and Spudich, 2002). When activated, Htr initiates a phosphorylation cascade that controls the directionality of the flagellar motor and directs phototaxis toward green and yellow light (SRI, peak absorption 587 nm) and away from blue light (SRII, peak absorption 487 nm) (Spudich, 2006; Spudich and Bogomolni, 1984). Given that prokaryotic kinase cascades are fundamentally different from eukaryotic second messengers (Scharf, 2010), opportunities to translate SR function to heterologous systems may be more complicated than with the ion pumps; such an effort could require reconstitution of the entire signal transduction cascade.

Light-Gated Ion Channels

ChRs are 7-TM proteins capable of conducting passive nonselective cation flow across the cellular membrane upon illumination and, in algae, also mediate intracellular signaling via a long C-terminal extension (Figure 1); for optogenetic applications, only the 7-TM ChR fragments are used, but in the native environment, the intracellular signaling activates a limited number of secondary ion channels that are seen as photocurrents at low light. In contrast, at high light intensities, the intrinsic conductances seen as short-delay currents are dominant and contribute up to 80% of the total current (Berthold et al., 2008; Ehlenbeck et al., 2002; Sineshchekov and Govorunova, 1999; Sineshchekov et al., 2002). A structural alignment of the 7-TM fragment (based solely on homology models) is shown in Figure 3A (BR and ChR2; note the polar residues that may contribute to the conducting pore. The recently discovered ChR1 of *Mesostigma viride* lacks two of the five anionic residues of this group, which might explain the small currents of this ChR in human embryonic kidney cells (Govorunova et al., 2011).
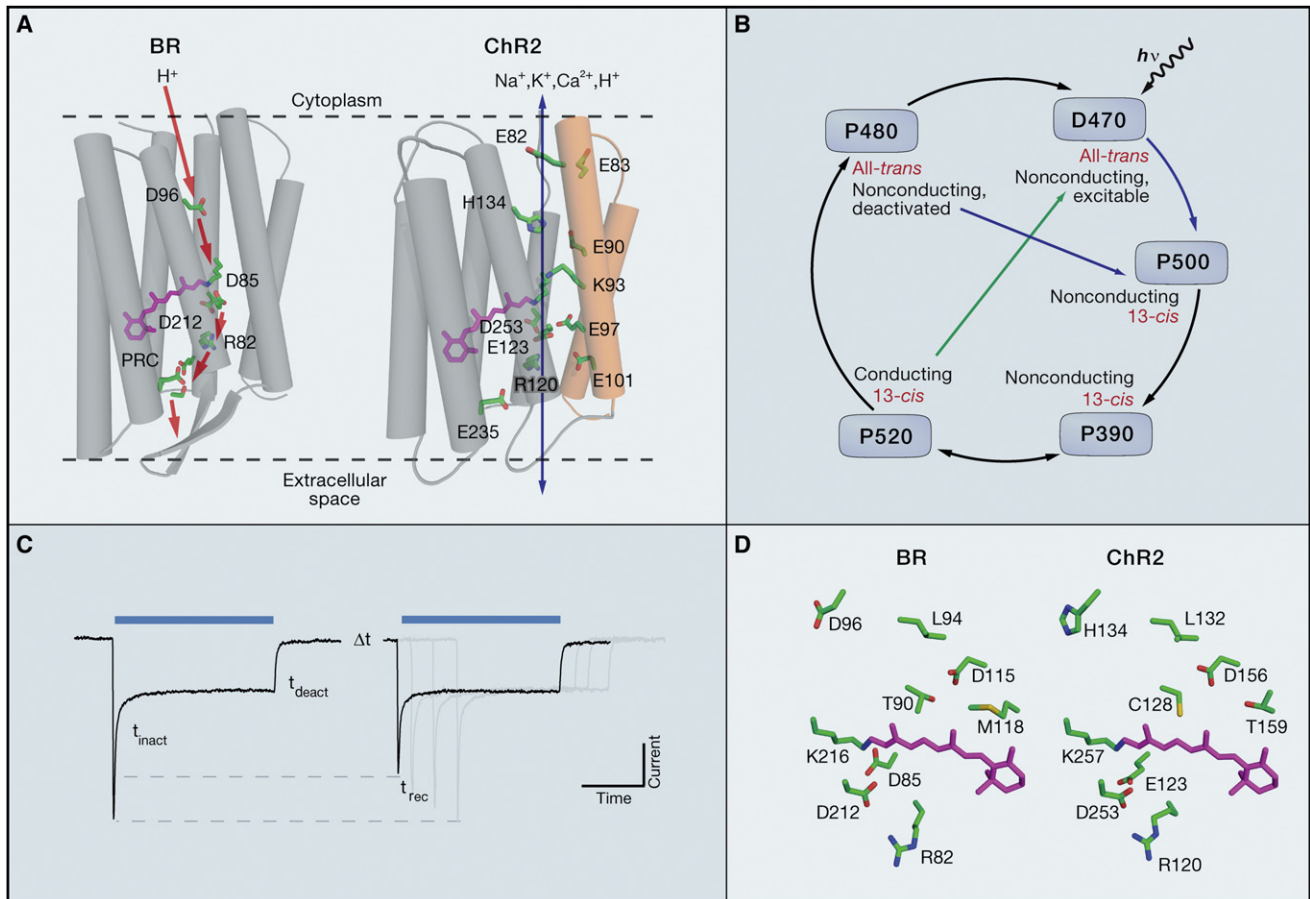
Figure 3. Structural and Functional Homology between BR and ChR
(A) Homology model-based structural alignment of ChR showing the 7-TM helices, next to the BR structural representation. For ChR2, the sequence of the illustrated residues may create a polar environment for water molecules and cation permeation. In BR, R82 functions as a connector between counterion and proton release complex, and D85 is the counterion to which the RSB proton is transferred. To emphasize the spatial discontinuity involved in pumping, only the proton transfer steps after photon absorption and proton transfer to D85 are shown.
(B) Simplified model for the photocycle of ChRs. The D470 dark state is converted by a light-induced isomerization of retinal via the early intermediate P500 and the transient P390 intermediate to the conducting-state P520. The recovery of the D470 dark state proceeds either thermally via the nonconducting P480 intermediate or photochemically via possible short-lived intermediates (green arrow). The late or desensitized P480 state can also be activated (blue arrow) to yield the early intermediate P500. Additional parallel cycles may be present (Yizhar et al., 2011b).
(C) Sample photocurrents show the key kinetic properties that govern function, including inactivation (*inact*), deactivation (*deact*), and recovery (*rec*).
(D) Homology near the retinal-binding pocket between BR and ChR2. The BR retinal-binding pocket is shown based on structure 1KGB (Facciotti et al., 2001) with key amino acids that are involved in the proton transfer reaction. The ChR residues are shown based on sequence homology in the relevant positions.

The first known and described ChR, channelrhodopsin-1 (ChR1), was identified as a light-gated ion channel in *Chlamydomonas reinhardtii*, a green unicellular alga from temperate freshwater environments (Nagel et al., 2002). Although originally considered proton selective (Nagel et al., 2002), later studies have found that ChR1 has broad cation conductance, including for Na^+, K^+, and even Ca^{2+} ions (Lin et al., 2009; Tsunoda and Hegemann, 2009). A second ChR, channelrhodopsin-2 (ChR2), was later characterized from the same organism (Figure 3B). Similar to ChR1, ChR2 also conducts cations (Nagel et al., 2003; Tsunoda and Hegemann, 2009), and both ChRs exhibit fast on and off kinetics. When introduced into neurons, ChRs can insert into the plasma membrane and mediate membrane potential changes in response to blue light (Boyden et al., 2005; Ishizuka et al., 2006; Li et al., 2005). Although ChR

expresses at higher levels than ChR1 in mammalian systems, a chimera of ChR1 with a ChR from another algal species, *Volvox carteri* (VChR1, described below), contains no ChR2 sequence elements yet generates significantly greater photocurrents than ChR2 (Yizhar et al., 2011b).

Both ChR1 and ChR2 bear sequence similarity to BR and other type I opsins, with strong homology in residues corresponding to the retinal-binding pocket and proton-conducting network (Hegemann et al., 2001; Nagel et al., 2002, 2003; Sineshchekov et al., 2002; Suzuki et al., 2003), suggesting that ChRs may share partially related ion conduction mechanisms with other microbial opsins. Indeed, the photocycle of ChR2 (Figure 3B) (Yizhar et al., 2011b) is similar to that of BR except with different spectral characteristics, likely due to variations in the ionic environment near the retinal Schiff base, larger conformational changes within

the protein (Radu et al., 2009; Ritter et al., 2008), and possibly higher water content within the proton network. In ChR2, a dark-adapted state absorbing at 470 nm (D470) converts rapidly upon illumination to the conducting state P520, via the short-lived photointermediates P500 and P390. Illumination of the open channel at this step with green light terminates the photocurrent (Bamann et al., 2008; Berndt et al., 2009) by photochemically shifting the channel back into a closed state, which may be the dark-adapted state D470 or the light-adapted state P480 (Stehfest and Hegemann, 2010), effectively resetting the photocycle. This photocycle-shortcut pathway may be relevant only at very high light intensities with wild-type ChR2 but acquires a special utility with certain molecularly engineered mutants known as step-function opsin genes (SFOs) with mutation in C128 (Berndt et al., 2009), which can essentially eliminate the inactivation and deactivation photocycle processes (Figures 3B–3D) and create bistable photocurrents.

Indeed, as with the light-activated ion pumps, molecular engineering and genomic strategies have begun to bear fruit for enhancing function of the light-activated ion channels and for understanding the mechanistic differences between rhodopsins that function as active pumps and passive channels. Molecular engineering has largely depended on molecular models derived from the available 3D structures of other microbial rhodopsins such as BR, HR, and SRII. The TM3 of ChRs contains residues important (Figure 3D) for controlling channel gating and the lifetime of the conducting state P520 (residues E123 and C128) and ion selectivity and competition (residues L132 and H134). The roles these residues play in ChR function are discussed in detail next.

Mechanistic Considerations

The most fundamental biophysical properties that influence the performance of opsins at the single-molecule level are efficiency of light absorption, which is dependent on both extinction coefficient (ε_{max} typically between 50,000 and 70,000 M^{-1} cm^{-1}) and quantum efficiency (Φ, typically between 0.3 and 0.7), and the turnover time of the photocycle. The latter is a critical parameter both for native function and for neuroscience application. For most light-driven pumps (HR and BR), the photocycle turnover time is ~10–20 ms, thereby capping the temporal precision at tens of milliseconds. Other opsin pumps such as blue PRs have much slower turnover time (~80–100 ms) (Wang et al., 2003) and therefore have limited applications for neuroscience. It is important to note that for most transporters, these values are determined at neutral membrane potential (0 mV), but the photocycle turnover time can be dramatically slower at hyperpolarized membrane potentials, extending from ~10–20 ms to ~100–400 ms (Geibel et al., 2001). Thus reductions in membrane potential slow down the pump, and more light is needed to achieve the same amount of hyperpolarization at more negative membrane potentials. In general, pump direction remains unchanged under all physiologically relevant conditions; the reported "pump inversion" phenomenon observed in PR is due to a leakiness of the pump under extremely negative voltages plus strong pH gradients (Lörinczi et al., 2009).

Unlike opsin-derived pumps, the kinetic parameters related to ChRs are determined by the efficiency of light absorption and the lifetime of the resulting conducting state, given that ion transport (down the gradients) is coupled to occupancy of the conducting state. The TM3 of ChRs contains key residues governing channel gating and the lifetime of the conducting state. The H134R point mutation in ChR2 (Figure 3D), homologous to the proton donor Asp96 in BR, increases the sodium conductance of ChR2 by ~2-fold; however temporal precision is significantly reduced due to slower deactivation kinetics (Gradinaru et al., 2007; Nagel et al., 2005). Another variant, ChR2-L132C (CatCH), has been shown to exhibit 1.6-fold more Ca^{2+} influx as well as reduced inactivation, which result together in 3-fold higher Ca^{2+} influx compared with wild-type ChR2 (Kleinlogel et al., 2011). And as noted above, modification of the C128 residue (C128S, C128A, C128T) in ChR2, alone or in combination with D156 (Berndt et al., 2009; Bamann et al., 2010; Yizhar et al., 2011b) (Figure 3D), extends the lifetime of the open state by several hundred- or even several thousand-fold and enables long-acting (step function-like) inward current in response to single pulses of light. This property leads to useful bistable behavior in the form of sustained subthreshold activation of neurons lasting up to many minutes (Berndt et al., 2009). Moreover, these variants in principle can achieve maximal current magnitudes similar to those in wild-type ChR2 but using much lower levels of light (Berndt et al., 2009; Schoenenberger et al., 2009; Yizhar et al., 2011b).

In addition to conducting-state lifetime, the unitary conductance of individual ChR molecules also affects performance. The single-channel conductance of ChR2 is estimated to be in the femtosiemens range; for order-of-magnitude estimation, in *Chlamydomonas* the integrated current in response to a half-saturating flash is carried by 1×10^6 ions (Harz et al., 1992), and with 10,000–120,000 ChRs per eyespot (Harz et al., 1992; Berthold et al., 2008; Govorunova et al., 2004) this would correspond to 10–100 ions per ChR and a single-channel conductance between 30 and 300 fS (Harz et al., 1992), a range that has been confirmed for ChR2 by noise analysis (Feldbauer et al., 2009; Lin et al., 2009). In this order-of-magnitude estimation we do not consider minority components from secondarily induced ionic currents that could be recruited, either in the native alga or in neurons under heterologous expression. We also note that it is not yet clear whether any ChR variants, identified by genomics or created by molecular engineering, have altered unitary conductance magnitude.

In addition to these single-molecule or intrinsic factors, population or extrinsic factors will also affect the functionality of microbial opsins, either in the native environment or when expressed in heterologous systems. Indeed, in order to achieve the highest levels of rhodopsin performance for experimental use, transcription, translation, folding, trafficking, and membrane targeting need to be optimized through a combination of codon optimization and addition of trafficking and targeting signals from the heterologous cellular host. TM helix shuffling may also prove influential; chimeras of ChR containing a combination of TMs from ChR1 and ChR2 (C1C2) (Lin et al., 2009; Tsunoda and Hegemann, 2009; Wang et al., 2009) or ChR1 and VChR1 (C1V1) (Yizhar et al., 2011a, 2011b) show reduced inactivation (as with ChR1) and also improved expression in mammalian cells.

In some cases, mutagenesis to achieve improved heterologous expression performance has also illuminated basic
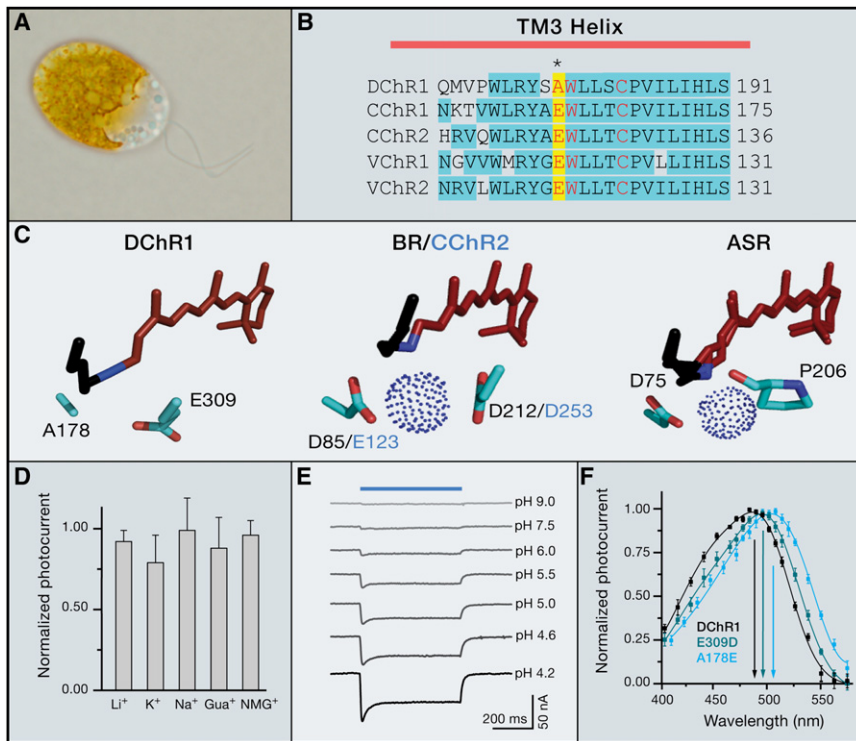
Figure 4. Characterization of a ChR from *Dunaliella salina*

(A) The halophilic unicellular alga *Dunaliella salina*.
(B) Sequence homology between the algal ChRs and BR within the third TM helix. The typically conserved E123 position has been replaced with an Ala in DChR1 (and is shown on a yellow background), conserved residues are shown on a blue background, and amino acids likely interacting with the chromophore are shown in red.
(C) Lack of a proton acceptor in DChR1 (A178), compared with BR (D85) and *Chlamydomonas* ChR2 (CChR2; E123). ASR (*Anabaena* sensory rhodopsin) has been crystallized with a mixture of all-*trans* and 13-*cis* retinal seen as an overlay (Vogeley et al., 2004).
(D) DChR1 photocurrents are unaffected by changes in the extracellular cation composition (sole cation present in each condition shown on category x axis). Cation exchange was performed in 5 mM Mops-NMG, 0.1 mM $MgCl_2$ with 100 mM LiCl, KCl, NaCl, guanidium chloride, or NMG chloride (pH 7.5). We used a human codon-adapted DChR sequence (amino acid residues 1–339) as a template for capped RNA synthesis by T7 RNA polymerase (mMessage mMachine, Ambion). Oocyte preparation and injection of capped RNA were carried out as described previously (Berthold et al., 2008), and two-electrode voltage clamp was performed with a Turbo Tec-05 (NPI Electronic) or a GeneClamp 500 (Molecular Devices) amplifier on an oocyte after 3–7 days of the capped RNA injection. Continuous light was provided by a 75-W Xenon lamp (Jena Instruments) and delivered to the oocytes via a 3 mm light guide. The light passed through a 500 ± 25 nm broadband filter (Balzers) with an intensity of 46 mW/cm².
(E) In contrast, DChR1 photocurrent is highly sensitive to changes in the pH environment. Solutions contained 100 mM NMG chloride, 0.1 mM $MgCl_2$, 0.1 mM $CaCl_2$ with 5 mM glycine (pH 9.0), 5 mM Mops-NMG (pH 7.5), 5 mM citrate (pH 6, 5.5, 5.0, 4.6, 4.2).
(F) Introduction or alteration of a proton acceptor (A178E or E309D) in the DChR1 retinal-binding pocket causes a pronounced red-shift in the absorption spectrum. We applied 10 ns laser flashes as described previously (Berthold et al., 2008); solutions for action spectra recording contained 100 mM NaCl, 0.1 mM $MgCl_2$, 0.1 mM $CaCl_2$, and 5 mM citrate (pH 4.2).

mechanisms of ChR function. For example, wild-type ChR2 exhibits a deactivation time constant after light-off of ∼10 ms and therefore can be used to drive neuronal firing at frequencies up to 40 to 50 Hz; however, achieving higher frequencies of neuronal firing requires faster formation and decay of the conducting state (P520 photocycle intermediate). Removal of the putative proton acceptor in the E123 position ("ChETA" mutation E123T or E123A; Figure 3D), at the residue that is homologous to D85 in BR, leads to more rapid channel closing and enables ultrafast optical control of spiking (at least up to 200 Hz; Gunaydin et al., 2010). The ChETA photocurrent is slightly smaller than wild-type ChR2 due to shorter open time, but this effect can be compensated for with more intense or longer flashes (for instance 2 ms instead of 1 ms) (Gunaydin et al., 2010). The E123A mutant therefore demonstrates that this residue, normally considered to be the proton acceptor, is not needed for any proton or other ion flux that would be an essential aspect of ChR function.
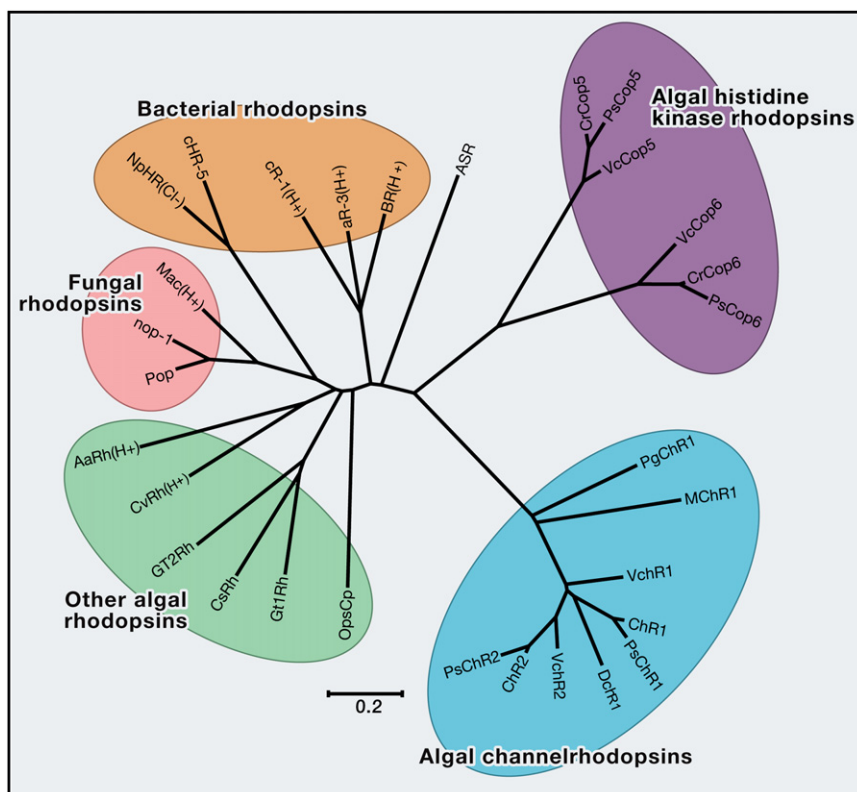
Outlook: Genome Mining and Molecular Engineering

It has been extraordinarily difficult to fundamentally alter ion selectivity or to generate useful action spectrum peak shifts of more than 10–20 nm (for ChRs that remain highly functional) by molecular engineering alone. Such efforts have generally failed, despite motivation to experimentally shift the action spectra of

ChRs in order to achieve combinatorial (multichannel) optical control, and despite clear understanding that the distribution of partial negative charges on either end of the all-*trans* retinal chromophore polyene will contribute to setting the wavelength of photons effectively absorbed.

However, using genomic analysis, in 2008 two new ChRs were reported from the colonial alga *Volvox carteri*, and one (VChR1) was found to absorb at markedly red-shifted wavelengths ($\lambda_{max} = 540$ nm; spiking could be driven even at 589 nm in hippocampal neurons) (Zhang et al., 2008). The expression level of VChR1 was found to be significantly lower than ChR2 in most host cells, although a slower decay of the open state partially compensated for the lower levels of protein expression (Zhang et al., 2008). The next few years witnessed steady improvement in VChR1, including TM domain shuffling, membrane-trafficking enhancement, and point mutations guided by structural models, culminating in the C1V1 family of ChRs (Yizhar et al., 2011b). C1V1 tools contain no ChR2 sequence but express more potent photocurrents than the original ChR2 and allow control of spiking with red light (e.g., 630 nm) and combinatorial excitation even in behaving mammals (Yizhar et al., 2011b).

The difficulty facing molecular engineering efforts highlights the value of crystal-structural information to allow more principled and accurate tuning (and understanding) of opsin properties and also underscores the value of genomic methods. Just as

replaced by Ala in the DChR1 TM3 (Figures 4B and 4C); from structural modeling (Figure 4C), we expect that the counterion function is assumed by E309 in DChR1, a position that plays only a minor role in BR (D212) or *Anabaena* sensory rhodopsin (ASR) (Vogeley et al., 2004). Even more remarkably, DChR1 photocurrents are exclusively carried by protons, unlike any other known ChR, and were completely unaffected by changes in the extracellular cation composition (Figure 4D). Consequently, the photocurrent was highly sensitive to changes in the pH environment and completely vanished at high pH (Figure 4E).

Full understanding of structure-function relationships will require high-resolution crystal structures in multiple photocycle states. However, directed mutagenesis studies here demonstrate that DChR1 has a different counterion arrangement and ion selectivity compared to other known ChRs. The strict H^+ selectivity of DChR1 was not mediated by the unusual RSBH counterion, as substitution of A178 with the more typical putative counterion Glu as found in ChR2 only red-shifted the activation spectrum (Figure 4F, from 475 to 510 nm) with minimal effect on current amplitude or kinetics. Similarly, replacing E309 with Asp caused a slight spectral shift and a slight current increase, whereas replacing the charged E309 by Ala rendered the protein almost totally inactive (Figure 4F).

Given typical electrochemical proton gradients, the DChR1 H^+ current is opposite in direction to the H^+ current generated by BR pump activity; therefore, DChR1 and BR could enable interventions such as bidirectional control of cellular pH, for example in manipulating the pH of intracellular compartments (mitochondria and synaptic vesicles). DChR1 therefore defines a new class of microbial opsin—a light-activated proton channel—unlike any other microbial opsin including ChR1 and ChR2. These findings illustrate the diversity of function likely to be present within the vast array of microbial opsin genomes.

To represent this diversity, in Figure 5 and Table 1 we have collected known microbial opsin sequences along with key properties and phylogenetic relationships and constructed a phylogenetic tree to display the primary sequence relationships among these distinct opsin genes. Although the development and application of microbial opsins as optogenetic tools has already

genome prospecting played an instrumental role in the identification of the new ChRs from *Volvox carteri*, genomic approaches could in principle be used to identify entirely new classes of opsins. Moreover, comparative analysis of opsins from the full range of ecological diversity could shed light on the fundamental mechanisms of ion selectivity, spectral tuning, and photocycle dynamics. To that end, we here report the identification of a panel of new ChRs from the genomes of the algae species *Pleodorina starrii*, *Pyramimonas gelidicola*, and *Dunaliella salina*; report that the *D. salina* ChR falls into a unique functional class (pure proton channel); and explore the theoretical and practical implications (Figures 4 and 5; Table 1).

Typically found in hyper-saline environments such as evaporation salt fields, the unicellular (oval with two flagella) green alga *Dunaliella salina* is salt tolerant. Despite belonging to the same order as the green algae *Chlamydomonas reinhardtii* and *Volvox carteri*, *Dunaliella* can appear reddish due to the accumulation of high levels of carotenoid molecules (Figure 4A). We hypothesized that a *Dunaliella* ChR might have unusual properties and engaged in efforts to clone ChRs from this flagellated algal species. Although we were only able to identify one opsin gene (DChR1) with homology to ChRs and VChRs from *Dunaliella* expressed sequence tags (ESTs), future work based on full genomic information may reveal additional DChRs.

Despite high homology with other known ChRs, the DChR1 sequence contained several notable features (Figure 4B). First, one of the residues that is thought to contribute to the complex counterion of the RSB, E123 in ChR2 as discussed above, is

Table 1. Phylogenetics of Microbial Opsins

Abbreviation	Name or Type	Species	Accession Number	Reference
Channelrhodopsin				
ChR1	channelrhodopsin-1	*Chlamydomonas reinhardtii*	AF385748	(Nagel et al., 2002)
ChR2	channelrhodopsin-2	*Chlamydomonas reinhardtii*	EF474017; AAM15777	(Nagel et al., 2003)
VChR1	channelrhodopsin-1	*Volvox carteri*	EU622855	(Zhang et al., 2008)
VChR2	channelrhodopsin-2	*Volvox carteri*	ABZ90903	(Kianianmomeni et al., 2009)
MChR1	channelrhodopsin-1	*Mesostigma viride*	JF922293	(Govorunova et al., 2011)
DChR1	channelrhodopsin-1	*Dunaliella salina*	JQ241364	present report
PsChR1	channelrhodopsin-1	*Pleodorina starrii*	JQ249903	present report
PsChR2	channelrhodopsin-2	*Pleodorina starrii*	JQ249904	present report
PgChR1	channelrhodopsin-1	*Pyramimonas gelidicola*	JQ241366	present report
Proton Pump				
AaRh	rhodopsin	*Acetabularia acetabulum*	AAY82897	(Tsunoda et al., 2006)
CvRh	rhodopsin	*Chlorella vulgaris*	JQ255360	present report
Gt1Rh	rhodopsin	*Guillardia theta*	ABA08437	(Sineshchekov et al., 2005)
GtR3	rhodopsin	*Guillardia theta*	JQ241365	(Gradinaru et al., 2010)
Pop	bacteriorhodopsin-like	*Podospora Anserine* S mat+	XP_001904282	(Espagne et al., 2008)
Mac	*L. Maculans* rhodopsin	*Leptosphaeria maculans*	AAG01180	(Idnurm and Howlett, 2001)
aR-3/Arch	archaerhodopsin-3	*Halorubrum sodomense*	BAA09452	(Ihara et al., 1999)
cR-1	cruxrhodopsin-1	*Haloarcula argentinensis*	BAA06678	(Tateno et al., 1994)
BR	bacteriorhodopsin	*Halobacterium salinarum*	CAA23744	(Dunn et al., 1981)
Cl⁻ Pump				
NpHR	halorhodopsin	*Natronomonas pharaonis*	EF474018	(Lanyi et al., 1990)
cHR-5	halorhodopsin	*Haloarcula marismortui* ATCC 43049	AAV46572	(Baliga et al., 2004)
Histidine Kinase Rhodopsin				
ASR	*Anabaena* sensory rhodopsin	*Anabaena sp.*	1XIO_A	(Vogeley et al., 2004)
CrCop5	chlamyopsin-5	*Chlamydomonas reinhardtii*	AAQ16277	(Kateriya et al., 2004)
CrCop6	chlamyopsin-6	*Chlamydomonas reinhardtii*	XP_001698789	(Kateriya et al., 2004)
VcCop5	volvoxopsin-5	*Volvox carteri*	XP_002954798	(Prochnik et al., 2010)
VcCop6	volvoxopsin-6	*Volvox carteri*	XP_002957065	(Prochnik et al., 2010)
PsCop5	pleopsin-5	*Pleodorina starri*	JQ249905	present report
PsCop6	pleopsin-6	*Pleodorina starri*	JQ249906	present report
Gt2Rh	rhodopsin-2	*Guillardia theta*	ABA08438	(Sineshchekov et al., 2005)
Other				
CsRh	rhodopsin	*Cryptomonas sp. S2*	ABA08439	(Sineshchekov et al., 2005)
OpsCp	rhodopsin	*Cyanophora paradoxa*	ACV05065	(Frassanito et al., 2010)
nop-1	rhodopsin-1	*Neurospora crassa* OR74A	XP_959421	(Bieszke et al., 1999)

profoundly improved our ability to perturb and understand biological systems, much remains to be learned regarding mechanisms by which these proteins respond to different light stimuli and select distinct ions for transport.

Indeed, as shown here, the microbial genomes continue to surprise and enrich us with fundamentally new optogenetic tools and capabilities. Continued investigation of this ecological diversity (Figure 5) and the functional phylogenetics of microbial opsins will enable the discovery and engineering of new variants with further wavelength-shifted absorption spectra and ion selectivity. Further rapid expansion of the optogenetic toolkit will in turn spur increased understanding of structure-function relationships and mechanisms of these ancient and powerful molecular machines.

SUPPLEMENTAL INFORMATION

Supplemental Information contains sequences and can be found with this article online at doi:10.1016/j.cell.2011.12.004.

REFERENCES

Airan, R.D., Thompson, K.R., Fenno, L.E., Bernstein, H., and Deisseroth, K. (2009). Temporally precise in vivo control of intracellular signalling. Nature *458*, 1025–1029.

Baliga, N.S., Bonneau, R., Facciotti, M.T., Pan, M., Glusman, G., Deutsch, E.W., Shannon, P., Chiu, Y., Weng, R.S., Gan, R.R., et al. (2004). Genome sequence of Haloarcula marismortui: a halophilic archaeon from the Dead Sea. Genome Res. *14*, 2221–2234.

Bamann, C., Kirsch, T., Nagel, G., and Bamberg, E. (2008). Spectral characteristics of the photocycle of channelrhodopsin-2 and its implication for channel function. J. Mol. Biol. *375*, 686–694.

Bamann, C., Gueta, R., Kleinlogel, S., Nagel, G., and Bamberg, E. (2010). Structural guidance of the photocycle of channelrhodopsin-2 by an interhelical hydrogen bond. Biochemistry *49*, 267–278.

Bamberg, E., Hegemann, P., and Oesterhelt, D. (1984). Reconstitution of halorhodopsin in black lipid membranes. Prog. Clin. Biol. Res. *164*, 73–79.

Béjà, O., Spudich, E.N., Spudich, J.L., Leclerc, M., and DeLong, E.F. (2001). Proteorhodopsin phototrophy in the ocean. Nature *411*, 786–789.

Berndt, A., Yizhar, O., Gunaydin, L.A., Hegemann, P., and Deisseroth, K. (2009). Bi-stable neural state switches. Nat. Neurosci. *12*, 229–234.

Berthold, P., Tsunoda, S.P., Ernst, O.P., Mages, W., Gradmann, D., and Hegemann, P. (2008). Channelrhodopsin-1 initiates phototaxis and photophobic responses in chlamydomonas by immediate light-induced depolarization. Plant Cell *20*, 1665–1677.

Bieszke, J.A., Braun, E.L., Bean, L.E., Kang, S., Natvig, D.O., and Borkovich, K.A. (1999). The nop-1 gene of Neurospora crassa encodes a seven transmembrane helix retinal-binding protein homologous to archaeal rhodopsins. Proc. Natl. Acad. Sci. USA *96*, 8034–8039.

Bogomolni, R.A., and Spudich, J.L. (1982). Identification of a third rhodopsin-like pigment in phototactic Halobacterium halobium. Proc. Natl. Acad. Sci. USA *79*, 6250–6254.

Boyden, E.S., Zhang, F., Bamberg, E., Nagel, G., and Deisseroth, K. (2005). Millisecond-timescale, genetically targeted optical control of neural activity. Nat. Neurosci. *8*, 1263–1268.

Büldt, G., Heberle, J., Dencher, N.A., and Sass, H.J. (1998). Structure, dynamics, and function of bacteriorhodopsin. J. Protein Chem. *17*, 536–538.

Chen, X., and Spudich, J.L. (2002). Demonstration of 2:2 stoichiometry in the functional SRI-HtrI signaling complex in Halobacterium membranes by gene fusion analysis. Biochemistry *41*, 3891–3896.

Chow, B.Y., Han, X., Dobry, A.S., Qian, X., Chuong, A.S., Li, M., Henninger, M.A., Belfort, G.M., Lin, Y., Monahan, P.E., and Boyden, E.S. (2010). High-performance genetically targetable optical neural silencing by light-driven proton pumps. Nature *463*, 98–102.

Deisseroth, K. (2011). Optogenetics. Nat. Methods *8*, 26–29.

Deisseroth, K., Feng, G., Majewska, A.K., Miesenböck, G., Ting, A., and Schnitzer, M.J. (2006). Next-generation optical technologies for illuminating genetically targeted brain circuits. J. Neurosci. *26*, 10380–10386.

Dunn, R., McCoy, J., Simsek, M., Majumdar, A., Chang, S.H., Rajbhandary, U.L., and Khorana, H.G. (1981). The bacteriorhodopsin gene. Proc. Natl. Acad. Sci. USA *78*, 6744–6748.

Ehlenbeck, S., Gradmann, D., Braun, F.J., and Hegemann, P. (2002). Evidence for a light-induced H(+) conductance in the eye of the green alga Chlamydomonas reinhardtii. Biophys. J. *82*, 740–751.

Espagne, E., Lespinet, O., Malagnac, F., Da Silva, C., Jaillon, O., Porcel, B.M., Couloux, A., Aury, J.M., Ségurens, B., Poulain, J., et al. (2008). The genome sequence of the model ascomycete fungus Podospora anserina. Genome Biol. *9*, R77.

Essen, L.O. (2002). Halorhodopsin: light-driven ion pumping made simple? Curr. Opin. Struct. Biol. *12*, 516–522.

Facciotti, M.T., Rouhani, S., Burkard, F.T., Betancourt, F.M., Downing, K.H., Rose, R.B., McDermott, G., and Glaeser, R.M. (2001). Structure of an early intermediate in the M-state phase of the bacteriorhodopsin photocycle. Biophys. J. *81*, 3442–3455.

Feldbauer, K., Zimmermann, D., Pintschovius, V., Spitz, J., Bamann, C., and Bamberg, E. (2009). Channelrhodopsin-2 is a leaky proton pump. Proc. Natl. Acad. Sci. USA *106*, 12317–12322.

Frassanito, A.M., Barsanti, L., Passarelli, V., Evangelista, V., and Gualtieri, P. (2010). A rhodopsin-like protein in Cyanophora paradoxa: gene sequence and protein immunolocalization. Cell. Mol. Life Sci. *67*, 965–971.

Geibel, S., Friedrich, T., Ormos, P., Wood, P.G., Nagel, G., and Bamberg, E. (2001). The voltage-dependent proton pumping in bacteriorhodopsin is characterized by optoelectric behavior. Biophys. J. *81*, 2059–2068.

Govorunova, E.G., Jung, K.H., Sineshchekov, O.A., and Spudich, J.L. (2004). Chlamydomonas sensory rhodopsins A and B: cellular content and role in photophobic responses. Biophys. J. *86*, 2342–2349.

Govorunova, E.G., Spudich, E.N., Lane, C.E., Sineshchekov, O.A., and Spudich, J.L. (2011). New channelrhodopsin with a red-shifted spectrum and rapid kinetics from Mesostigma viride. MBio *2*, e00115–e11.

Gradinaru, V., Thompson, K.R., Zhang, F., Mogri, M., Kay, K., Schneider, M.B., and Deisseroth, K. (2007). Targeting and readout strategies for fast optical neural control in vitro and in vivo. J. Neurosci. *27*, 14231–14238.

Gradinaru, V., Thompson, K.R., and Deisseroth, K. (2008). eNpHR: a Natronomonas halorhodopsin enhanced for optogenetic applications. Brain Cell Biol. *36*, 129–139.

Gradinaru, V., Zhang, F., Ramakrishnan, C., Mattis, J., Prakash, R., Diester, I., Goshen, I., Thompson, K.R., and Deisseroth, K. (2010). Molecular and cellular approaches for diversifying and extending optogenetics. Cell *141*, 154–165.

Gunaydin, L.A., Yizhar, O., Berndt, A., Sohal, V.S., Deisseroth, K., and Hegemann, P. (2010). Ultrafast optogenetic control. Nat. Neurosci. *13*, 387–392.

Harz, H., Nonnengasser, C., and Hegemann, P. (1992). The photoreceptor current of the green alga chlamydomonas. Philos. Trans. R. Soc. Lond. B Biol. Sci. *338*, 39–52.

Haupts, U., Tittor, J., Bamberg, E., and Oesterhelt, D. (1997). General concept for ion translocation by halobacterial retinal proteins: the isomerization/switch/transfer (IST) model. Biochemistry *36*, 2–7.

Hegemann, P., Fuhrmann, M., and Kateriya, S. (2001). Algal sensory photoreceptors. J. Phycol. *37*, 668–676.

Hildebrand, E., and Dencher, N. (1975). Two photosystems controlling behavioural responses of Halobacterium halobium. Nature *257*, 46–48.

Idnurm, A., and Howlett, B.J. (2001). Characterization of an opsin gene from the ascomycete Leptosphaeria maculans. Genome *44*, 167–171.

Ihara, K., Umemura, T., Katagiri, I., Kitajima-Ihara, T., Sugiyama, Y., Kimura, Y., and Mukohata, Y. (1999). Evolution of the archaeal rhodopsins: evolution rate changes by gene duplication and functional differentiation. J. Mol. Biol. *285*, 163–174.

Ishizuka, T., Kakuda, M., Araki, R., and Yawo, H. (2006). Kinetic evaluation of photosensitivity in genetically engineered neurons expressing green algae light-gated channels. Neurosci. Res. *54*, 85–94.

Kateriya, S., Nagel, G., Bamberg, E., and Hegemann, P. (2004). "Vision" in single-celled algae. News Physiol. Sci. 19, 133–137.

Kianianmomeni, A., Stehfest, K., Nematollahi, G., Hegemann, P., and Hall-mann, A. (2009). Channelrhodopsins of Volvox carteri are photochromic proteins that are specifically expressed in somatic cells under control of light, temperature, and the sex inducer. Plant Physiol. 151, 347–366.

Kim, J.M., Hwa, J., Garriga, P., Reeves, P.J., RajBhandary, U.L., and Khorana, H.G. (2005). Light-driven activation of beta 2-adrenergic receptor signaling by a chimeric rhodopsin containing the beta 2-adrenergic receptor cytoplasmic loops. Biochemistry 44, 2284–2292.

Kleinlogel, S., Feldbauer, K., Dempski, R.E., Fotis, H., Wood, P.G., Bamann, C., and Bamberg, E. (2011). Ultra light-sensitive and fast neuronal activation with the $Ca^{2}+$-permeable channelrhodopsin CatCh. Nat. Neurosci. 14, 513–518.

Kolbe, M., Besir, H., Essen, L.O., and Oesterhelt, D. (2000). Structure of the light-driven chloride pump halorhodopsin at 1.8 A resolution. Science 288, 1390–1396.

Kralj, J.M., Douglass, A.D., Hochbaum, D.R., Maclaurin, D., and Cohen, A.E. (2011). Optical recording of action potentials in mammalian neurons using a microbial rhodopsin. Nat. Methods. Published online November 27, 2011. 10.1038/nmeth.1782.

Lanyi, J.K. (2004). Bacteriorhodopsin. Annu. Rev. Physiol. 66, 665–688.

Lanyi, J.K., Duschl, A., Hatfield, G.W., May, K., and Oesterhelt, D. (1990). The primary structure of a halorhodopsin from Natronobacterium pharaonis. Structural, functional and evolutionary implications for bacterial rhodopsins and halorhodopsins. J. Biol. Chem. 265, 1253–1260.

Li, X., Gutierrez, D.V., Hanson, M.G., Han, J., Mark, M.D., Chiel, H., Hegemann, P., Landmesser, L.T., and Herlitze, S. (2005). Fast noninvasive activation and inhibition of neural and network activity by vertebrate rhodopsin and green algae channelrhodopsin. Proc. Natl. Acad. Sci. USA 102, 17816–17821.

Lin, J.Y., Lin, M.Z., Steinbach, P., and Tsien, R.Y. (2009). Characterization of engineered channelrhodopsin variants with improved properties and kinetics. Biophys. J. 96, 1803–1814.

Lörinczi, E., Verhoefen, M.K., Wachtveitl, J., Woerner, A.C., Glaubitz, C., Engelhard, M., Bamberg, E., and Friedrich, T. (2009). Voltage- and pH-dependent changes in vectoriality of photocurrents mediated by wild-type and mutant proteorhodopsins upon expression in Xenopus oocytes. J. Mol. Biol. 393, 320–341.

Luecke, H., Schobert, B., Richter, H.T., Cartailler, J.P., and Lanyi, J.K. (1999). Structure of bacteriorhodopsin at 1.55 A resolution. J. Mol. Biol. 291, 899–911.

Man, D., Wang, W., Sabehi, G., Aravind, L., Post, A.F., Massana, R., Spudich, E.N., Spudich, J.L., and Béjà, O. (2003). Diversification and spectral tuning in marine proteorhodopsins. EMBO J. 22, 1725–1731.

Marwan, W., and Oesterhelt, D. (1987). Signal formation in the halobacterial photophobic response mediated by a fourth retinal protein (P480). J. Mol. Biol. 195, 333–342.

Matsuno-Yagi, A., and Mukohata, Y. (1977). Two possible roles of bacteriorhodopsin; a comparative study of strains of Halobacterium halobium differing in pigmentation. Biochem. Biophys. Res. Commun. 78, 237–243.

Michel, H., and Oesterhelt, D. (1976). Light-induced changes of the pH gradient and the membrane potential in H. halobium. FEBS Lett. 65, 175–178.

Nagel, G., Ollig, D., Fuhrmann, M., Kateriya, S., Musti, A.M., Bamberg, E., and Hegemann, P. (2002). Channelrhodopsin-1: a light-gated proton channel in green algae. Science 296, 2395–2398.

Nagel, G., Szellas, T., Huhn, W., Kateriya, S., Adeishvili, N., Berthold, P., Ollig, D., Hegemann, P., and Bamberg, E. (2003). Channelrhodopsin-2, a directly light-gated cation-selective membrane channel. Proc. Natl. Acad. Sci. USA 100, 13940–13945.

Nagel, G., Brauner, M., Liewald, J.F., Adeishvili, N., Bamberg, E., and Gottschalk, A. (2005). Light activation of channelrhodopsin-2 in excitable cells of Caenorhabditis elegans triggers rapid behavioral responses. Curr. Biol. 15, 2279–2284.

Oesterhelt, D., and Stoeckenius, W. (1971). Rhodopsin-like protein from the purple membrane of Halobacterium halobium. Nat. New Biol. 233, 149–152.

Oesterhelt, D., Hegemann, P., and Tittor, J. (1985). The photocycle of the chloride pump halorhodopsin. II: Quantum yields and a kinetic model. EMBO J. 4, 2351–2356.

Oh, E., Maejima, T., Liu, C., Deneris, E., and Herlitze, S. (2010). Substitution of 5-HT1A receptor signaling by a light-activated G protein-coupled receptor. J. Biol. Chem. 285, 30825–30836.

Palczewski, K., Kumasaka, T., Hori, T., Behnke, C.A., Motoshima, H., Fox, B.A., Le Trong, I., Teller, D.C., Okada, T., Stenkamp, R.E., et al. (2000). Crystal structure of rhodopsin: A G protein-coupled receptor. Science 289, 739–745.

Prochnik, S.E., Umen, J., Nedelcu, A.M., Hallmann, A., Miller, S.M., Nishii, I., Ferris, P., Kuo, A., Mitros, T., Fritz-Laylin, L.K., et al. (2010). Genomic analysis of organismal complexity in the multicellular green alga Volvox carteri. Science 329, 223–226.

Racker, E., and Stoeckenius, W. (1974). Reconstitution of purple membrane vesicles catalyzing light-driven proton uptake and adenosine triphosphate formation. J. Biol. Chem. 249, 662–663.

Radu, I., Bamann, C., Nack, M., Nagel, G., Bamberg, E., and Heberle, J. (2009). Conformational changes of channelrhodopsin-2. J. Am. Chem. Soc. 131, 7313–7319.

Ritter, E., Stehfest, K., Berndt, A., Hegemann, P., and Bartl, F.J. (2008). Monitoring light-induced structural changes of Channelrhodopsin-2 by UV-visible and Fourier transform infrared spectroscopy. J. Biol. Chem. 283, 35033–35041.

Sakmar, T.P. (2002). Structure of rhodopsin and the superfamily of seven-helical receptors: the same and not the same. Curr. Opin. Cell Biol. 14, 189–195.

Scharf, B., and Engelhard, M. (1994). Blue halorhodopsin from Natronobacterium pharaonis: wavelength regulation by anions. Biochemistry 33, 6387–6393.

Scharf, B.E. (2010). Summary of useful methods for two-component system research. Curr. Opin. Microbiol. 13, 246–252.

Schobert, B., and Lanyi, J.K. (1982). Halorhodopsin is a light-driven chloride pump. J. Biol. Chem. 257, 10306–10313.

Schoenenberger, P., Gerosa, D., and Oertner, T.G. (2009). Temporal control of immediate early gene induction by light. PLoS ONE 4, e8185.

Schröder-Lang, S., Schwärzel, M., Seifert, R., Strünker, T., Kateriya, S., Looser, J., Watanabe, M., Kaupp, U.B., Hegemann, P., and Nagel, G. (2007). Fast manipulation of cellular cAMP level by light in vivo. Nat. Methods 4, 39–42.

Shichida, Y., and Yamashita, T. (2003). Diversity of visual pigments from the viewpoint of G protein activation—comparison with other G protein-coupled receptors. Photochem. Photobiol. Sci. 2, 1237–1246.

Sineshchekov, O.A., and Govorunova, E.G. (1999). Rhodopsin-mediated photosensing in green flagellated algae. Trends Plant Sci. 4, 58–63.

Sineshchekov, O.A., Jung, K.H., and Spudich, J.L. (2002). Two rhodopsins mediate phototaxis to low- and high-intensity light in Chlamydomonas reinhardtii. Proc. Natl. Acad. Sci. USA 99, 8689–8694.

Sineshchekov, O.A., Govorunova, E.G., Jung, K.H., Zauner, S., Maier, U.G., and Spudich, J.L. (2005). Rhodopsin-mediated photoreception in cryptophyte flagellates. Biophys. J. 89, 4310–4319.

Spudich, J.L. (1998). Variations on a molecular switch: transport and sensory signalling by archaeal rhodopsins. Mol. Microbiol. 28, 1051–1058.

Spudich, J.L. (2006). The multitalented microbial sensory rhodopsins. Trends Microbiol. 14, 480–487.

Spudich, J.L., and Bogomolni, R.A. (1984). Mechanism of colour discrimination by a bacterial sensory rhodopsin. Nature 312, 509–513.

Spudich, J.L., Yang, C.S., Jung, K.H., and Spudich, E.N. (2000). Retinylidene proteins: structures and functions from archaea to humans. Annu. Rev. Cell Dev. Biol. 16, 365–392.

Stehfest, K., and Hegemann, P. (2010). Evolution of the channelrhodopsin photocycle model. ChemPhysChem *11*, 1120–1126.

Stierl, M., Stumpf, P., Udwari, D., Gueta, R., Hagedorn, R., Losi, A., Gärtner, W., Petereit, L., Efetova, M., Schwarzel, M., et al. (2011). Light modulation of cellular cAMP by a small bacterial photoactivated adenylyl cyclase, bPAC, of the soil bacterium Beggiatoa. J. Biol. Chem. *286*, 1181–1188.

Suzuki, T., Yamasaki, K., Fujita, S., Oda, K., Iseki, M., Yoshida, K., Watanabe, M., Daiyasu, H., Toh, H., Asamizu, E., et al. (2003). Archaeal-type rhodopsins in Chlamydomonas: model structure and intracellular localization. Biochem. Biophys. Res. Commun. *301*, 711–717.

Takahashi, T., Mochizuki, Y., Kamo, N., and Kobatake, Y. (1985). Evidence that the long-lifetime photointermediate of s-rhodopsin is a receptor for negative phototaxis in Halobacterium halobium. Biochem. Biophys. Res. Commun. *127*, 99–105.

Tamura, K., Peterson, D., Peterson, N., Stecher, G., Nei, M., and Kumar, S. (2011). MEGA5: molecular evolutionary genetics analysis using maximum likelihood, evolutionary distance, and maximum parsimony methods. Mol. Biol. Evol. *28*, 2731–2739.

Tateno, M., Ihara, K., and Mukohata, Y. (1994). The novel ion pump rhodopsins from Haloarcula form a family independent from both the bacteriorhodopsin and archaerhodopsin families/tribes. Arch. Biochem. Biophys. *315*, 127–132.

Tomioka, H., Takahashi, T., Kamo, N., and Kobatake, Y. (1986). Flash spectrophotometric identification of a fourth rhodopsin-like pigment in Halobacterium halobium. Biochem. Biophys. Res. Commun. *139*, 389–395.

Tsunoda, S.P., and Hegemann, P. (2009). Glu 87 of channelrhodopsin-1 causes pH-dependent color tuning and fast photocurrent inactivation. Photochem. Photobiol. *85*, 564–569.

Tsunoda, S.P., Ewers, D., Gazzarrini, S., Moroni, A., Gradmann, D., and Hegemann, P. (2006). H+ -pumping rhodopsin from the marine alga Acetabularia. Biophys. J. *91*, 1471–1479.

Váró, G., Brown, L.S., Lakatos, M., and Lanyi, J.K. (2003). Characterization of the photochemical reaction cycle of proteorhodopsin. Biophys. J. *84*, 1202–1207.

Vogeley, L., Sineshchekov, O.A., Trivedi, V.D., Sasaki, J., Spudich, J.L., and Luecke, H. (2004). Anabaena sensory rhodopsin: a photochromic color sensor at 2.0 A. Science *306*, 1390–1393.

Wang, H., Sugiyama, Y., Hikima, T., Sugano, E., Tomita, H., Takahashi, T., Ishizuka, T., and Yawo, H. (2009). Molecular determinants differentiating photocurrent properties of two channelrhodopsins from chlamydomonas. J. Biol. Chem. *284*, 5685–5696.

Wang, W.W., Sineshchekov, O.A., Spudich, E.N., and Spudich, J.L. (2003). Spectroscopic and photochemical characterization of a deep ocean proteorhodopsin. J. Biol. Chem. *278*, 33985–33991.

Witten, I.B., Lin, S.C., Brodsky, M., Prakash, R., Diester, I., Anikeeva, P., Gradinaru, V., Ramakrishnan, C., and Deisseroth, K. (2010). Cholinergic interneurons control local circuit activity and cocaine conditioning. Science *330*, 1677–1681.

Yizhar, O., Fenno, L.E., Davidson, T.J., Mogri, M., and Deisseroth, K. (2011a). Optogenetics in neural systems. Neuron *71*, 9–34.

Yizhar, O., Fenno, L.E., Prigge, M., Schneider, F., Davidson, T.J., O'Shea, D.J., Sohal, V.S., Goshen, I., Finkelstein, J., Paz, J.T., et al. (2011b). Neocortical excitation/inhibition balance in information processing and social dysfunction. Nature *477*, 171–178.

Yoshitsugu, M., Yamada, J., and Kandori, H. (2009). Color-changing mutation in the E-F loop of proteorhodopsin. Biochemistry *48*, 4324–4330.

Zhang, F., Wang, L.P., Boyden, E.S., and Deisseroth, K. (2006). Channelrhodopsin-2 and optical control of excitable cells. Nat. Methods *3*, 785–792.

Zhang, F., Aravanis, A.M., Adamantidis, A., de Lecea, L., and Deisseroth, K. (2007a). Circuit-breakers: optical technologies for probing neural signals and systems. Nat. Rev. Neurosci. *8*, 577–581.

Zhang, F., Wang, L.P., Brauner, M., Liewald, J.F., Kay, K., Watzke, N., Wood, P.G., Bamberg, E., Nagel, G., Gottschalk, A., and Deisseroth, K. (2007b). Multimodal fast optical interrogation of neural circuitry. Nature *446*, 633–639.

Zhang, F., Prigge, M., Beyrière, F., Tsunoda, S.P., Mattis, J., Yizhar, O., Hegemann, P., and Deisseroth, K. (2008). Red-shifted optogenetic excitation: a tool for fast neural control derived from Volvox carteri. Nat. Neurosci. *11*, 631–633.

Zhang, F., Gradinaru, V., Adamantidis, A.R., Durand, R., Airan, R.D., de Lecea, L., and Deisseroth, K. (2010). Optogenetic interrogation of neural circuits: technology for probing mammalian brain structures. Nat. Protoc. *5*, 439–456.